



OPEN

No effects of 1 Hz offline TMS on performance in the stop-signal game

Maximilian A. Friehs^{1,3,6}✉, Julia Siodmiak^{1,5}, Michelle C. Donzallaz⁴, Dora Matzke⁴, Ole Numssen¹, Christian Frings² & Gesa Hartwigen^{1,7}

Stopping an already initiated action is crucial for human everyday behavior and empirical evidence points toward the prefrontal cortex playing a key role in response inhibition. Two regions that have been consistently implicated in response inhibition are the right inferior frontal gyrus (IFG) and the more superior region of the dorsolateral prefrontal cortex (DLPFC). The present study investigated the effect of offline 1 Hz transcranial magnetic stimulation (TMS) over the right IFG and DLPFC on performance in a gamified stop-signal task (SSG). We hypothesized that perturbing each area would decrease performance in the SSG, albeit with a quantitative difference in the performance decrease after stimulation. After offline TMS, functional short-term reorganization is possible, and the domain-general area (i.e., the right DLPFC) might be able to compensate for the perturbation of the domain-specific area (i.e., the right IFG). Results showed that 1 Hz offline TMS over the right DLPFC and the right IFG at 110% intensity of the resting motor threshold had no effect on performance in the SSG. In fact, evidence in favor of the null hypothesis was found. One intriguing interpretation of this result is that within-network compensation was triggered, canceling out the potential TMS effects as has been suggested in recent theorizing on TMS effects, although the presented results do not unambiguously identify such compensatory mechanisms. Future studies may result in further support for this hypothesis, which is especially important when studying reactive response in complex environments.

Stopping before a crosswalk when the traffic light suddenly changes to red or not telling the joke you planned to tell after realizing it's not appropriate are a few of the many examples of effective response inhibition in everyday situations. Inhibitory control is one part of cognitive control that, by effective suppression of behavior after initiation, allows one to navigate through a constantly changing environment and is fundamental for daily well-being and sometimes survival. Inhibitory control is generally conceptualized as a capacity to suppress one's own unwanted actions, thoughts, or feelings after recognizing them as currently undesired. This mechanism is key to select appropriate responses, suppress irrelevant stimuli and achieve relevant goals¹. Deficits in inhibitory control are common in neurological patients diagnosed with Alzheimer's, Parkinson's or frontal lobe lesions²⁻⁴, as well as patients with depression, mania, obsessive compulsive disorder (OCD) and patients fighting obesity⁵⁻⁷. Although attention-deficit hyperactivity disorder (ADHD) and schizophrenia are frequently associated with decreased inhibitory control, these effects may also be due to impairments in early attentional processes^{8,9}. Impaired inhibitory control may lead to impulsive behavior and intrusive, ruminating thoughts and is considered a factor increasing the likelihood of addiction and acts of aggression. There are many ways of measuring inhibitory control but the stop signal task (SST) is arguably one of the most widely used paradigms to study reactive inhibitory control in the laboratory¹⁰.

Studying inhibitory control with the stop signal task. In the standard SST, participants are required to press a specific button whenever a cue (an arrow pointing left or right) is presented on a screen unless a "stop" cue is presented after the first one, indicating that participants must refrain from any reaction, hence inhibiting

¹Lise-Meitner Research Group Cognition and Plasticity, Max Planck Institute for Human Cognitive and Brain Sciences, Leipzig, Germany. ²Department of General Psychology and Methodology, Trier University, Trier, Germany. ³School of Psychology, University College Dublin, Dublin, Ireland. ⁴Department of Psychology, Psychological Methods Unit, University of Amsterdam, Amsterdam, The Netherlands. ⁵University of Gdansk, Gdańsk, Poland. ⁶Psychology of Conflict Risk and Safety, University of Twente, Enschede, The Netherlands. ⁷Wilhelm Wundt Institute for Psychology, Leipzig University, Leipzig, Germany. ✉email: m.a.friehs@utwente.nl; friehs@cbs.mpg.de

it. They are instructed to respond as quickly as possible and the time difference between “go” and “stop” cues, called Signal-stop-delay (SSD), differs making it easier or harder to withhold the response. Performance in this task is highly variable among the healthy population and often reaches abnormally low scores in patients with poor action inhibition. To quantify individual performance, both speed and accuracy are considered and the time to successfully stop the initiated action is calculated based on participants’ performance estimating the stop-signal reaction Time (SSRT)^{11,12}. As the Stop-Signal task is based on an independent race model¹³, in which the cognitive process of “go” reaction and “stop” reaction are two separate processes, whichever process reaches completion first, determines the resulting behavior. Accordingly, earlier completion of the go process results in failure to inhibit a response while earlier completion of the “stop” process leads to successful response inhibition. The SSRT reflects the latency of the stop process, i.e. how quickly a response can be stopped.

However, while the SST is commonly used in lab-based research, it also has its drawbacks and can be monotonous for participants. Recently, several research teams have developed gamified stop-signal tasks^{14,15}, which do not change the underlying architecture of the SST but yield more enjoyable experiences for participants. Further, these gamified tasks provide a more engaging environment which creates a more captivating setting that may aid in collecting data from populations with a lower attention span such as children or groups of patients with concentration or attention deficits^{16–19}.

The neurophysiological underpinnings of response inhibition. Neuroimaging studies in the past have identified key brain areas and circuits for executive processes. One of the largest brain areas associated with cognitive control is the prefrontal cortex (PFC), postulated as a center of control processes already by Luria in 1962 (for a recent version see Luria, 2012²⁰). In particular, response inhibition processes are associated with activity in the dorsolateral prefrontal cortex (DLPFC) and the right inferior frontal gyrus (IFG)^{21–24}. Hinting at their general relevance in the cognitive control network, both DLPFC and IFG are also implicated in other complex cognitive processes such as error detection and conflict resolution²⁵.

The DLPFC is further associated with working memory as well as selective attention²⁶ and can be activated during emotional regulation processes^{27,28} to exert top-down influence on emotional reactivity²⁹. It is also involved in conscious decision making, outcome prediction and, of course, inhibition³⁰. Lesion studies show that DLPFC damage leads to less efficient response inhibition during the stop-signal task². One key assumption is that the prefrontal cortex does not act independently, but rather changes the actions and signals from other areas, and the resulting cognitive control stems from active goal maintenance; a process closely connected to DLPFC activity²⁴. The DLPFC may be viewed as a more domain general processing area involved in a multitude of cognitive processes, such as working memory and emotional or memory suppression, as evidenced by overlapping activation within the area in several different tasks^{23,26,31}. Further, DLPFC activity has been shown to be, for example, connected with food-related impulsivity and risk-taking behavior further indicating that the right DLPFC is involved in executive functioning on a domain general level^{32,33}.

Studies investigating right IFG activity consistently implicate the area in response inhibition tasks^{34,35}. Further, lesion studies provide additional evidence for a direct link of the right IFG and response inhibition³⁶. However, some studies suggest that the rIFG is not only active during response inhibition, but also during target detection tasks^{35,37}. This fits recent evidence from a lesion study suggesting that the rIFG is partially responsible for detecting salient signals (such as stop-signals), leading to the triggering of an inhibitory control process³⁸. The rIFG is connected with the pre-SMA, an important area for voluntary action inhibition. Specifically, it has been proposed that the rIFG acts as ‘emergency break’ when the need to stop an action arises^{21,39–41}. Thus, the right IFG can be conceptualized as a domain specific processing area, responsible for motor response inhibition^{21,42}.

The involvement of specific brain areas in the response inhibition process can be directly probed with non-invasive brain stimulation procedures. Although some previous studies have used transcranial magnetic stimulation (TMS) over the right PFC to modulate response inhibition in the SST, the results are heterogeneous and the interaction of the specific subregions within the right PFC (i.e., rDLPFC and rIFG) and their individual contributions to the response inhibition process remains unclear. Specifically, stimulation over the right IFG can lead to a performance deficit in the SST^{43–45} or no effect at all⁴⁶. Even fewer studies investigated TMS effects over the right DLPFC on response inhibition in the SST and the results show no effect of TMS on the response inhibition process even though the prevailing theory suggests that perturbation of that area should impact performance^{22,44,47}.

The present study

The goal of the present study was to investigate the impact of offline TMS (i.e., applied before task processing) over the right IFG and DLPFC on performance in a gamified stop-signal task. The stop-signal game (SSG) is a recently developed and validated adaptation of the SST, in which participants have to navigate through an enchanted forest¹⁴. The task functions analogous to the SST and is characterized by increased visual demands due to the everchanging 3D images on screen. Importantly, previous research demonstrated that performance between a standard SST and the SSG is comparable, while the SSG is considered more enjoyable for participants¹⁴. In this study, participants underwent three experimental sessions with either a real stimulation over the IFG or DLPFC or sham TMS. We hypothesized that perturbation of either area would decrease performance in the SSG. However, we expected a quantitative difference in the performance decrease after stimulation. After offline TMS, functional reorganization is possible and the domain-general area (i.e., the right DLPFC) might be able to compensate for the perturbation of the domain-specific area (i.e., the right IFG). Put differently, the effects of TMS on SSG performance were hypothesized to be smaller in the rIFG stimulation condition than in the rDLPFC stimulation condition.

Results

Overall, performance was in the expected range, and comparable to previous studies utilizing a similar gamified task version^{14,15,48–50}. For details see Table 1.

SSRT. Results of a 6 (Order) × 3 (TMS Condition: rDLPFC vs. rIFG vs. sham) repeated measures ANOVA showed neither a significant main effect of TMS Condition ($F(2, 34) = 0.186, p = 0.83$), nor a main effect of Order ($F(5, 17) = 1.4, p = 0.27$) nor an interaction ($F(10, 34) = 0.432, p = 0.93$). For a visual representation see Fig. 1. We included order as a between-subjects factor in the analysis to control for potential sequence effects. Further, complementary Bayesian analysis revealed a $BF_{01} = 6.94$ in favor of the null-hypothesis with regards to the main effect of TMS Condition. We used a Cauchy prior distribution with $r = 0.707$ since this prior reflects the range of most psychological effects⁵¹. Bayesian analysis was done with JASP Version 0.17.1 (JASP Team 2023).

Error rates. A 6 (Order) × 3 (TMS Condition: rDLPFC vs. rIFG vs. sham) repeated measures ANOVA revealed no main effect of TMS Condition ($F(2, 34) = 0.13, p = 0.88$), and no main effect of Order ($F(5, 17) = 0.32$,

	rDLPFC	rIFG	Sham
SSRT	453 (57)	456 (50)	458 (52)
SSD	520 (233)	500 (191)	483 (185)
Correct Go-RT	999 (215)	974 (176)	964 (156)
p(response inhibition)	0.48 (0.027)	0.47 (0.021)	0.48 (0.022)
Overall go-accuracy	0.99 (0.019)	98 (0.036)	0.98 (0.022)

Table 1. Descriptive performance data depending on the TMS condition. Standard deviations shown in brackets. SSRT, SSD and Correct Go-RT are shown in milliseconds and overall accuracy in percent.

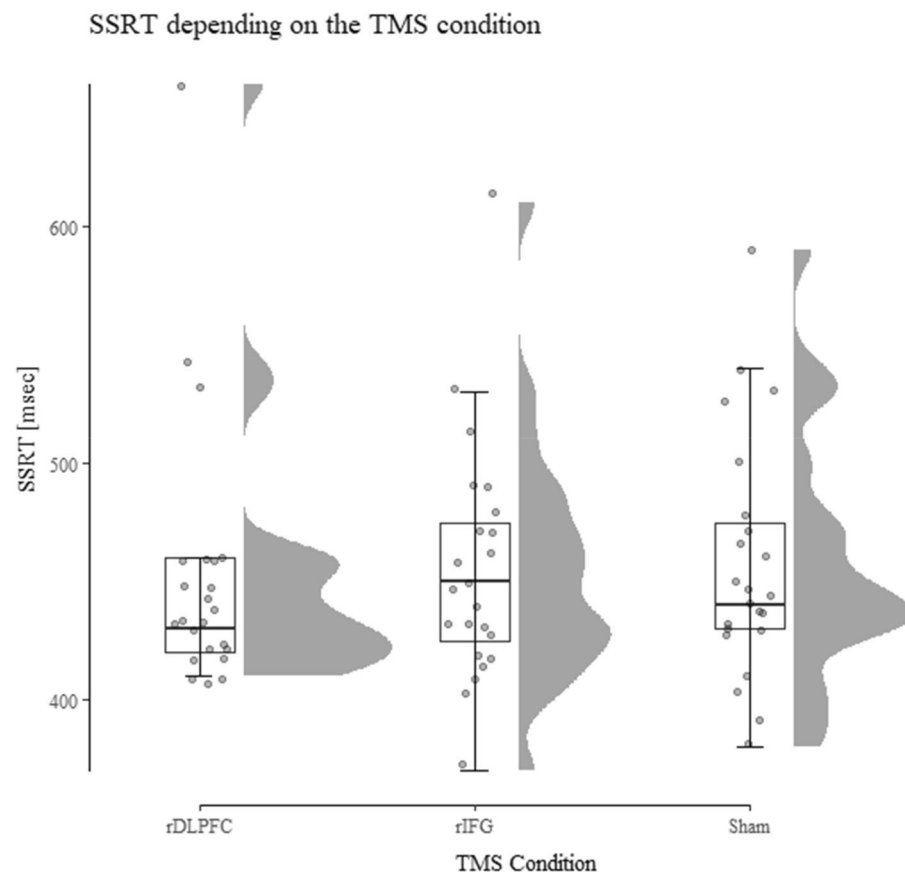


Figure 1. SSRT by TMS Condition as computed by the integration method. Results show no difference in SSRT depending on the TMS Condition. SSRT on the y-axis is displayed in msec. Descriptively, the variance in the rDLPFC condition is lower compared to the other conditions.

$p=0.89$) or an interaction ($F(10, 34)=1.52, p=0.17$). Further, complementary Bayesian analysis revealed a $BF_{01}=7.20$ in favor of the null-hypothesis with regards to the main effect TMS Condition.

SSD. A 6 (Order) \times 3 (TMS Condition: rDLPFC vs. rIFG vs. sham) repeated measures ANOVA revealed neither a main effect of TMS Condition ($F(2, 34)=1.88, p=0.17$), nor a main effect of Order ($F(5, 17)=2.05, p=0.12$) nor an interaction ($F(10, 34)=0.92, p=0.53$). Further, complementary Bayesian analysis reveals a $BF_{01}=2.18$ in favor of the null-hypothesis with regards to the main effect TMS condition.

Go RT. Results of a 6 (Order) \times 3 (TMS Condition: rDLPFC vs. rIFG vs. sham) repeated measures ANOVA showed neither significant main effect of TMS Condition ($F(2, 34)=2.13, p=0.13$), nor a main effect of Order ($F(5, 17)=1.97, p=0.34$) nor an interaction ($F(10, 34)=0.87, p=0.57$). Further, complementary Bayesian analysis reveals a $BF_{01}=2.39$ in favor of the null-hypothesis with regards to the main effect TMS Condition.

Bayesian modeling results. The population-level parameters from the hierarchical model were estimated as location and scale parameters but transformed into means and standard deviations before interpreting them. The go and stop trigger failure parameters were estimated on the real line and were transformed back to the probability scale using a bivariate inverse probit transformation. We used the means of the transformed posterior distributions as point estimates. To quantify posterior uncertainty, we computed 95% credible intervals (i.e., the 2.5th and 97.5th percentile of the posterior samples). Table 2 shows the posterior means and corresponding credible intervals of the population-level model parameters across conditions. To compute the posterior distribution of mean Go-RT and SSRT, we summed up the independent MCMC samples for the respective μ and τ parameters on each iteration and collapsed them across chains.

Parameter differences between conditions were explored using pairwise Bayesian p-values (BP). BPs denote the proportion of posterior samples that is greater than the posterior samples in the comparison condition. If a BP is close to 1 or 0, the posterior distribution of the comparison condition is shifted to lower or higher values, respectively, which suggests that the parameter of interest differs between conditions. The pairwise BPs for SSRT ranged from 0.239 to 0.426, for correct Go-RT, from 0.285 to 0.42, for trigger failures from 0.26 to 0.4, and for go failures from 0.304 to 0.407, overall indicating greatly overlapping posterior distributions and hence no reliable differences (see Fig. 2).

Discussion

In this study, we probed the functional relevance of the right IFG and right DLPFC for reactive response inhibition. We observed no effect of 1 Hz offline rTMS over either brain area on performance. Importantly, there was no TMS effect with neither standard frequentist methods, nor with Bayesian modeling analyses. In fact, SSRT estimates—the most important performance measure—differed on average only by a few milliseconds between conditions and the posterior distributions showed a large degree of overlap. Especially the mean SSRT posterior distributions of the sham and the rIFG stimulation conditions and the individual SSRTs, as computed by the integration method, look almost identical (see Figs. 1, 2), whereas the posterior distribution for rDLPFC was slightly shifted towards lower SSRT; however that minor shift was far from reliable.

Further, Bayesian modeling revealed no difference between the stimulation conditions with regards to stop or go trigger failure probability, indicating that the present null result in SSRT cannot be attributed to differences in the likelihood of launching the stop and go processes. Recent research provided evidence for a higher degree of trigger failures and a slower SSRT (mainly carried in μ_{stop}) in rIFG lesion patients³⁸. Consequently, it would have been plausible to assume that disruption via TMS to the rIFG would lead to a similar pattern of results. With that being said, it is unclear what exact results pattern would be expected for a successful disruption of the rDLPFC.

Although we expected a performance disruption after stimulation, these results overall fit the heterogeneous results in the literature. For example, while Chambers et al.⁴⁴ found no effect of 15 min of 1 Hz at, on average, 92% distance-adjusted RMT over the right DLPFC (for a similar result see also Upton et al.⁴⁷), they did observe

	rDLPFC	rIFG	Sham
μ_{go}	0.897 [0.799, 0.992]	0.872 [0.799, 0.946]	0.868 [0.803, 0.935]
σ_{go}	0.097 [0.075, 0.123]	0.094 [0.074, 0.117]	0.099 [0.076, 0.128]
τ_{go}	0.102 [0.083, 0.123]	0.104 [0.082, 0.127]	0.099 [0.078, 0.121]
Correct Go-RT $\mu_{go} + \tau_{go}$	0.999 [0.901, 1.10]	0.976 [0.9, 1.06]	0.967 [0.897, 1.04]
μ_{stop}	0.415 [0.396, 0.435]	0.417 [0.402, 0.433]	0.411 [0.397, 0.427]
σ_{stop}	0.038 [0.027, 0.051]	0.036 [0.025, 0.051]	0.036 [0.026, 0.050]
τ_{stop}	0.036 [0.025, 0.051]	0.043 [0.03, 0.06]	0.052 [0.036, 0.073]
SSRT $\mu_{stop} + \tau_{stop}$	0.452 [0.429, 0.475]	0.461 [0.44, 0.483]	0.463 [0.442, 0.488]
P(GF)	0.012 [0.005, 0.028]	0.014 [0.006, 0.032]	0.018 [0.006, 0.043]
P(TF)	0.056 [0.024, 0.118]	0.047 [0.023, 0.085]	0.059 [0.037, 0.092]

Table 2. Posterior means of model parameters and their 95% credible intervals. SSRT and Go-RT are shown in seconds. Go and Trigger failures, P(GF) and P(TF), are shown as probabilities.

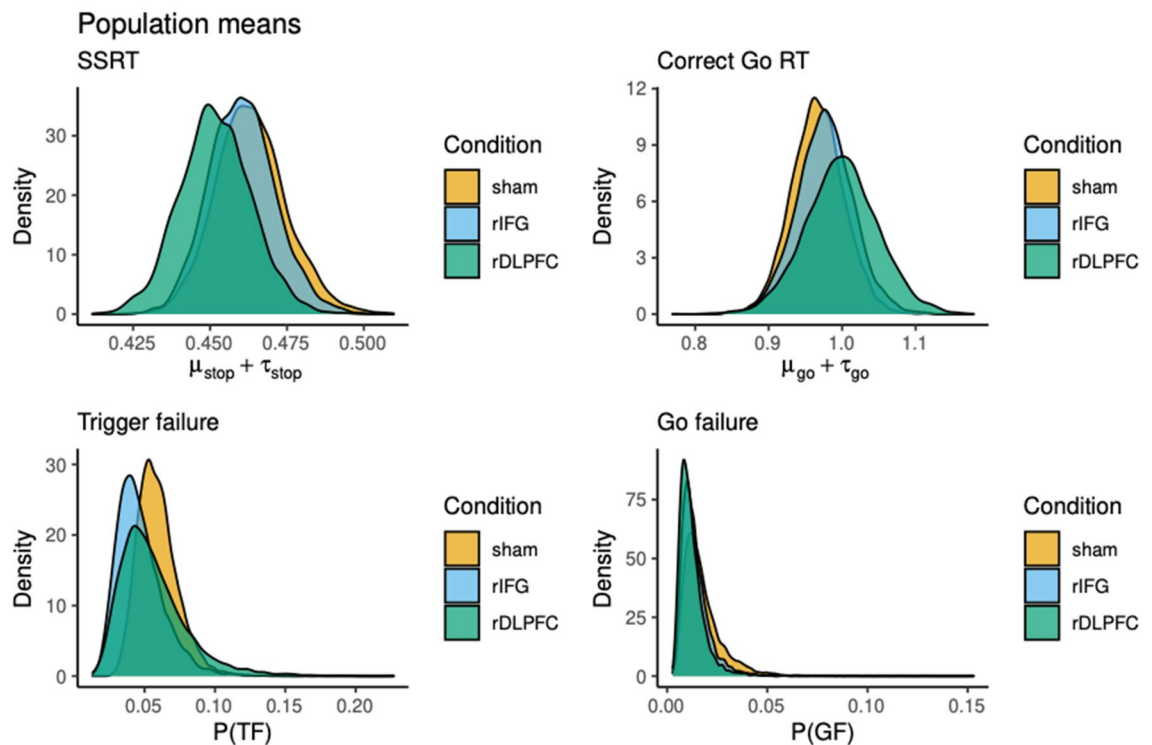


Figure 2. Posterior distributions of the population-level mean parameters across conditions. *SSRT* stop-signal reactiontime, *RT* Response time, *P(TF)* stop trigger failure probability, *P(GF)* go trigger failure probability. *SSRT* and *Correct Go RT* are on the millisecond scale, stop and go trigger failures are on the probability scale.

a perturbation after right IFG stimulation (see also Lee et al.⁴⁶). In another study, offline continuous theta burst stimulation yielded a behavioral effect on performance after stimulating the right anterior insula, close to the right IFG, but no effect after right middle frontal gyrus stimulation²².

There are several factors that may contribute to the null-effects in the present study besides compensatory mechanisms as well as the heterogeneous results in the literature. First, although TMS is among the more precise NIBS methods, without previous functional MRI it is not possible to ensure that each person is stimulated in exactly the right area and neuronal activity in non-target regions may be modulated instead. Second, not all brain areas make for equally good targets and stimulation spreads to neighboring cortical areas depending on the individuals' brain anatomy⁵². Third, there are large interindividual differences with regards to TMS- and more generally NIBS-effects on performance^{53,54}. Apart from the difference in neuroanatomy, there are also baseline activity differences to be considered and some authors report on a brain state dependent stimulation effects^{55,56}. This inter- and even intra-individual variability to TMS may mask potential TMS effects and increase the likelihood of null-results and a non-significant result may not necessarily equate to an absence of effect. Fourth, different TMS protocols impact the type of inference that is possible. Thus for example, while online interference protocols (e.g., 10 Hz rTMS in short bursts during stimulus processing) cause a disruption of an ongoing task, offline inhibition protocols (e.g., 1 Hz TMS or cTBS before task performance) are assumed to decrease cortical excitability via presumably long-term depression of the stimulated synapses⁵⁴. Fifth, given the possibility of short-term cortical reorganization it may be possible that the lack of TMS effect on performance may be due to within-network compensation^{54,57}. Put differently, it is possible, or even likely, that 1 Hz TMS over one area led to an up-regulation of another area which helped to compensate for the perturbation. Given the duration of the stimulation and the fact that no TMS was applied during task performance, this compensation effect could have nullified any potential TMS effect. These lines of reasoning and results also fit with recent transcranial direct current stimulation (tDCS) studies^{58–60}. However, compensation of TMS-based perturbation is not always possible and compensatory mechanisms may break down when cognitive demands are especially high⁶¹ or due to their inherent asymmetry. Specifically, domain-general areas may be able to compensate for disturbance in process-specific areas but compensation of domain-general area disruption by domain-specific areas is less likely^{57,62–64}.

The ability of the human brain to flexibly reorganize processes to changing situations and task requirements and to compensate for perturbations is astonishing⁵⁷. For example, some research suggests that an upregulation of regions associated with the domain-general network can drive language recovery after lesions to specialized language areas in aphasia patients^{63,65}. It has further been suggested that the brain is primed for neuroplasticity after a stroke, which can lead to heightened effectiveness of rehabilitative therapy^{66,67}. Thus, the fact that we did not observe a TMS effect on performance may suggest a potential compensatory effect that future studies may probe. There are several factors that may contribute to the null-effects in the present study besides compensatory mechanisms as well as the heterogeneous results in the literature. First, although TMS is among the more precise NIBS methods, without previous functional MRI, it is not possible to ensure that each person is stimulated in

exactly the right area and neuronal activity in non-target regions may be modulated instead⁵⁴. Second, not all brain areas are equally suitable targets and stimulation can spread to neighboring cortical areas, both of which can impact stimulation outcomes⁵². Third, there are large interindividual differences with regards to TMS—and more generally NIBS-effects—on performance^{53,54}. Apart from differences in neuroanatomy, baseline performance and activity differences should also be considered, which may lead to a brain-state dependent stimulation effects^{55,56}. Such inter- and even intra-individual variability to TMS may mask potential TMS effects and increase the likelihood of null-results. Consequently, a non-significant result may not necessarily equate to the absence of an effect. However, baseline differences are usually ignored in TMS studies⁶⁸. With that being said, although Bayesian analyses cannot overcome these challenges, they can provide evidence for the null hypothesis. Accordingly, our complementary Bayesian analysis revealed moderate evidence in favor of the null (for Bayes Factor interpretation see Lee and Wagenmakers, 2014⁶⁹). Fourth, different TMS protocols may differentially impact task performance. For example, while online interference protocols (e.g., 10 Hz rTMS in short bursts during stimulus processing) can result in a disruption of ongoing task performance, offline inhibition protocols (e.g., 1 Hz TMS or cTBS before task performance) are assumed to decrease cortical excitability, presumably via long-term depression-like effects on the stimulated synapses⁵⁴. Fifth, given the possibility of short-term cortical reorganization, it is possible that the lack of a clear TMS effect on performance may be due to within-network compensation^{54,57}.

There are several possible avenues for future research on the prefrontal inhibition network. For example, researchers may utilize a condition-and-perturb protocol to probe compensatory mechanisms within the right prefrontal cortex. Here, a combined offline and online perturbation of both the right IFG and right DLPFC may result in stronger effects relative to the perturbation of each area alone, which would allow testing the compensation theory. Additionally, researchers may aim to increase stimulation focality by targeting individual activation peaks based on functional localizers obtained from fMRI. Recent advances even allow for the concurrent use of TMS and neuroimaging procedures^{70,71}.

Another limitation of the current study is the specific sham condition that was used. To reiterate, the coil was placed on a participant's head and tilted away to avoid effective cortical stimulation during TMS. A more ideal sham procedure would have been to place the coil directly on the vertex or even stimulate a control site assumed to not be part of the network required for task performance^{54,72–74}. In this way, a more realistic sham condition could have mimicked the somatosensory side effects of TMS. However, while this procedural change would have generally improved the study design, it is unlikely that an active sham condition would have turned the observed null findings into positive effects. Notably, by more closely mimicking the somatosensory effects an active sham condition may slightly reduce the likelihood of finding an active TMS effect in comparison by creating a placebo effect⁷². However, although we cannot fully rule out this possibility, the present study employed an offline TMS protocol and any somatosensory effect of an active TMS application would have most likely faded and not affected the task after its cessation.

Conclusion

In conclusion, 1 Hz offline TMS over the right DLPFC and the right IFG at 110% RMT had no effect on performance in a gamified SST. In fact, evidence in favor of the null hypothesis was found. However it needs to be noted that the BEESTS model cannot prove the null, and evidence for the null hypothesis is based on SSRT estimates via the integration method. One theoretically intriguing interpretation of this result is that within-network compensation was triggered canceling out the potential TMS effects as has been suggested in recent theorizing on TMS effects.

Methods

Sample. 27 participants were recruited via the database of Max Planck Institute for Human Cognitive and Brain Sciences, Leipzig, Germany. Written informed consent was obtained from each subject prior to the experiment. The study was approved by the local ethics committee of the Medical Faculty at Leipzig University. All participants were healthy right-handed volunteers aged between 18 and 40, had normal or corrected-to-normal vision, no cardiovascular, neurological or psychiatric disorders or metal implants. Participants were informed about procedures but were blinded regarding the different TMS conditions. Based on the data reduction criteria (see below) the final sample consisted of 23 participants (14 female, mean age = 30.17, SD = 5.4). For sample size estimations and power analysis, we assumed an effect of Cohen's $f = 0.4$ for a TMS effect on SSRT, a medium sized correlation between measures of $r = 0.5$ and a Type I and Type II error of 0.05 (using GPower⁷⁵). This calculation resulted in a sample of at least 18 participants. Further, this sample size is in line with previous research investigating stop-signal task performance. For example, some studies similar to the present study in terms of design employed samples sized between 8 and 24^{22,44,46,47}.

Design. Each participant underwent three experimental sessions that varied in TMS site (rIFG vs. rDLPFC vs. sham). After preparation and a practice block, each participant performed 450 experimental trials of the SSG per session, split into nine blocks. Each session lasted approximately 1.5–2.5 h. The individual resting motor threshold was determined in the first session. Sessions were separated by at least 7 days to prevent carry-over effects. The order of sessions was counterbalanced across participants to the best possible degree. Our design resulted in six possible stimulation sequences.

Transcranial magnetic stimulation. We applied 30 min of neuronavigated 1 Hz TMS (TMS Navigator, Localite, Sankt Augustin, Germany) prior to the SSG (i.e., offline TMS). 30 min of 1 Hz TMS has been shown to decrease regional cerebral glucose metabolic rates as evidenced by PET scans⁷⁶ and influenced various cognitive

processes such as action reprogramming and memory formation^{77–79}. Moreover, effects appear to be intensity-dependent, with higher intensities leading to a stronger effect^{80,81}. The stimulation was based on co-registered individual T1-weighted MR images to navigate the TMS coil and maintain its exact location and orientation throughout all sessions. T1-weighted images were taken from the in-house database or acquired at a 3-Tesla MRI (Prisma, Siemens Healthcare, Germany) using a magnetization prepared rapid gradient echo (MPRAGE) sequence in sagittal orientation (inversion time=650 ms, repetition time=300 ms, flip angle=10°, field of view=256 mm × 240 mm, voxel-size=1 mm × 1 mm × 1.5 mm). TMS was performed using the average Montreal Neurological Institute (MNI) coordinates for the rIFG ($x=50, y=19, z=16$) and rDLPFC ($x=40, y=32, z=36$) based on previous studies and meta-analysis^{22,34,43,44,46,82–86}. Note that the exact labeling of these prefrontal areas is inconsistent across studies and the reported activation peaks and stimulation sites are heterogeneous. Individual stimulation targets for rIFG and rDLPFC were obtained by using the inverted normalization procedure in SPM 8 (Wellcome Trust Center for Neuroimaging, University College London, UK) to transform the MNI coordinates to individual space. Sham TMS was applied over the vertex, which was determined as the midpoint between the lines connecting the nasion andinion and tragi of the left and right ear. At the beginning of each experimental session, participants were co-registered to their structural T1. Individual resting motor thresholds (rMTs) were determined in the first session^{61,87}. Stimulation intensity was set to 110% of the participant's rMT⁴⁷. The coil was placed tangentially on the head with the handle pointing at 45° to the sagittal plane for both active TMS conditions. A figure-of-eight coil (CB-60; double 60 mm) connected to a MagPro X100 stimulator (MagVenture, Denmark) was used, and the overall application of TMS pulses was within recommended safety limits^{88,89}. During the individual session, the coil was held in place by the experimenter. Accurate coil positioning and maintenance were achieved with a neuronavigation system, which was placed behind the participant but visible to the experimenter. Participants were asked to lean against a custom-made headrest with the back of their head and avoid movements during the experiment. All participants tolerated this procedure and completed the whole experiment. Note that in case of discomfort we reduced the stimulation intensity by 1–2%. Specifically, in 8 out of 46 active sessions a reduction of at most 2% maximum stimulator output (MSO) was needed. Further, 3 participants (i.e. 6 active sessions) required a reduction in both active stimulation conditions. Note that the average stimulation intensity was 110.48% (SD = 1.05) for the rDLPFC and 110.49% (SD = 1.01) for the rIFG. For the sham condition, the coil was oriented parallel to the sagittal plane and placed across the vertex. Importantly, the coil was tilted away from the head in the sham condition to avoid any effective stimulation of the underlying brain tissue; in this case only the rim of the coil touched the participants' head.

To validate stimulation conditions, we performed post-hoc electrical field simulations of the TMS-induced electric fields for the rDLPFC and rIFG conditions. We used SimNIBS v3.2.6 to construct high-resolution geometric head models^{90,91} from individual MRI data (Puonti et al., 2016), employing SPM12 and CAT12⁹² and to estimate individual field exposures via the finite element method (FEM). The final head models were composed of $\sim 1.7 \times 10^6$ nodes and $\sim 9.5 \times 10^6$ tetrahedra. T1 images and, if available, T2 images were used for segmenting the following tissues: scalp, skull, grey matter (GM), white matter (WM), cerebrospinal fluid (CSF), and eyes. Standard conductivity values for the tissue types were used. We utilized the coil positions saved by the neuronavigation software to define the position and orientation of the TMS coil for the field simulations^{93,94}. We visually assessed the individual field simulations to assure effective stimulation of the cortical targets and differential stimulation patterns across the TMS conditions. Figure 3 shows the e-field simulations of an exemplary subject.

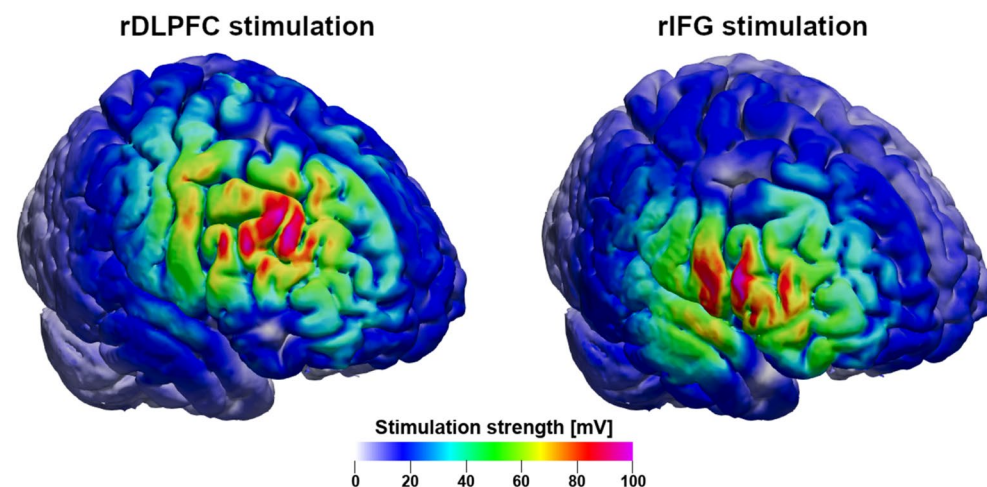


Figure 3. Both cortical sites were effectively targeted with TMS. The stimulation exposed the cortical target (left: rDLPFC; right: rIFG) to significant electrical stimulation. Critically, the off-target regions, including the alternative target, were stimulated significantly less (green areas) than the cortical target. Color: overall stimulation strength $|E|$, shown on a grey matter surface for an exemplary subject. Simulation was performed with realistic parameters, i.e., 110% rMT intensity and CB-60 coil model.

Task. Response inhibition was measured using a validated stop-signal game that is conceptually identical to the ordinary SST^{14,48}. The SSG is a 3D game in the infinite runner genre, in which the participant has to navigate a character through an enchanted forest. Importantly, the SSG retains measurement validity and exhibits the same properties as the regular SST, apart from an increase in visual complexity and being generally more enjoyable for participants. This is in line with evidence that game-like elements such as simple narratives and consequential choices enhance motivation^{95,96}. Mirroring the ordinary SST exactly, but enhancing ecological validity through visual complexity, the SSG required the participants to react to a visual stimulus (i.e., left or right pointing fairy sprite on the screen); on a random subset of trials an auditory stop-signal (i.e., beep-sound) was presented, which required subjects to withhold their already initiated response. Figure 4 illustrates the SSG. In each trial, the go-stimulus was presented for a maximum of 2000 ms or until the response. The stop-signal was presented via headphones following a variable delay (the Stop-Signal Delay, SSD). The SSD represents the delay between the onset of the go- and the stop-signal and was initially set to 250 ms. The SSD was continuously adjusted with a staircase procedure to obtain a probability of responding of 50%. After the reaction was successfully stopped (i.e., button press was inhibited), the SSD was increased by 50 ms, whereas when the participants did not stop successfully, the SSD was decreased by 50 ms. The inter-trial interval was set to a random value between 500 and 1500 ms. Several different performance measures were logged and calculated, including the SSD and the probability of making a (wrong) response when a stop-signal was presented ($p(\text{response}|\text{signal})$). Furthermore, two variables that are directly related to accuracy were logged: first, the number of *omission errors* (reflecting the probability of missed responses on go-trials) and second, the number of *commission errors* (reflecting the probability of an incorrect response on go-trials). Additionally, we logged three RT variables; *correct go RT* reflects the speed of correct responses on trials without a stop signal, *incorrect go RT* reflects the response time of wrong go responses (i.e., pressing left when a right turn would have been required or vice versa) and *signal response RT*, which indicates the latency of the incorrectly executed response on stop-signal trials. Furthermore, the probability of a *correct inhibition* (i.e., the likelihood of inhibiting an already initiated action) was recorded for each participant. Most importantly, the stop-signal reaction time (SSRT) could be calculated based on a participant's

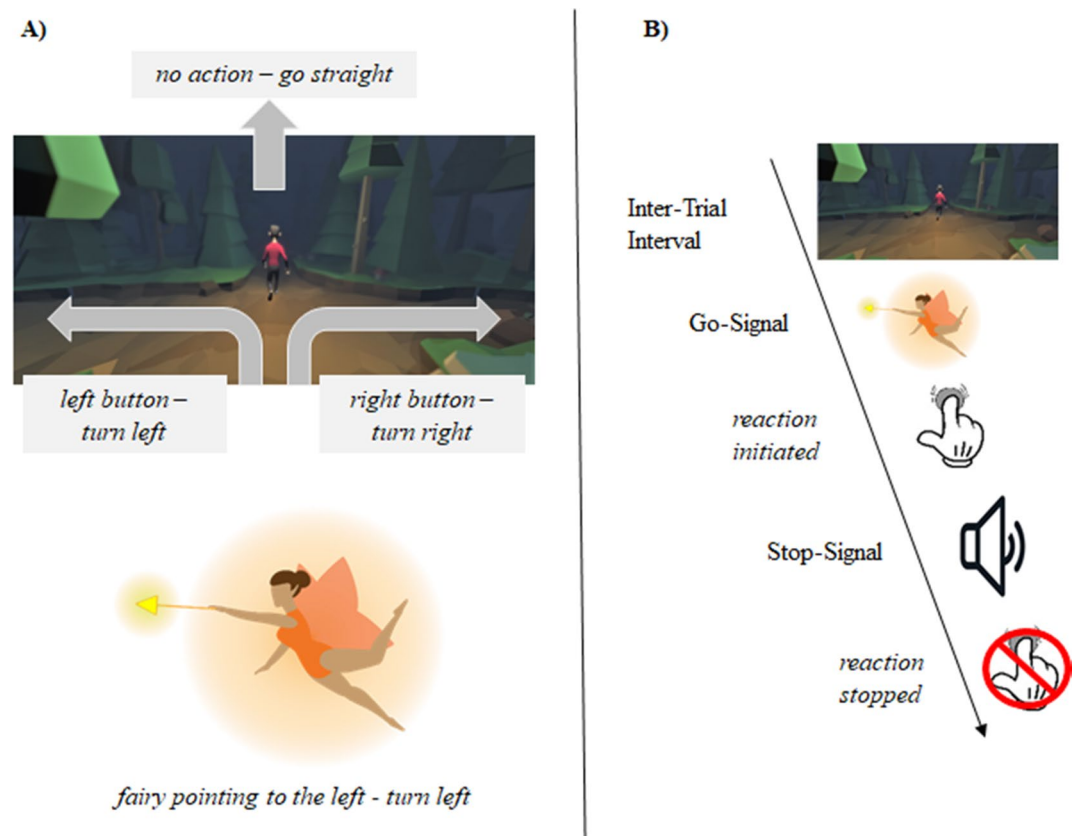


Figure 4. Visualization of the Stop-Signal Game. (A) The picture on top shows the basic layout of the SSG environment. The character runs through a procedurally generated forest and has the option to turn left or right at each upcoming intersection. If no button is pressed and no direction is chosen, the character will continue to run straight ahead. The picture on the bottom shows representation of the basic go-stimulus that is used in the SSG. The fairy appears at each intersection and either points to the left or to the right. (B) A prototypical trial in the SSG. During the inter-trial interval the avatar will move through the forest on its own. At an intersection a go-signal in the form of a fairy would appear to indicate the direction the participant should press on the keyboard. After a variable delay, an auditory stop-signal may be presented on a subsection of trials after which a participant should withhold their already initiated action.

performance. The estimation of the SSRT was based on the integration method with replacement of omissions as well as on hierarchical Bayesian parametric modeling^{8,10,97}.

Data reduction. Only participants with three valid datasets (i.e., participated in all three sessions and provided analysable data) were considered for the final analysis. Thus, 3 participants with incomplete datasets were excluded at this stage. In accordance with the recommendations in the literature^{10,12}, we screened participants' performance data in the SSG to make sure that reactive inhibition is accurately estimated. This included testing for the horse-race model assumption by comparing *signal response RT* (i.e., wrongly executed responses on stop-trial) and go RT. The horse-race model dictates that SSRT can only reliably be estimated if mean signal response RT is faster than mean go RT. Further, we will show that there is a statistical difference between the average go-RT (i.e., RTs of correct responses during go-trials) and the average signal response RT (i.e., RTs of false responses during stop-trials) for each experimental condition. Furthermore, we checked whether participants' $p(\text{response}|\text{signal})$ was lower than 0.25 or higher than 0.75 or if their accuracy on go-trials was an outlier based on the Tukey outlier criterion. Additionally, we screened participants' performance for strategic response behavior, based on which we excluded data from one participant (e.g., nearly uniformly distributed RT data). Furthermore, we removed anticipatory responses (i.e., responses faster than 0.2 s; $n=2$).

Bayesian parametric modeling. The data was modeled using BEESTS, a Bayesian parametric approach for the analysis of stop-signal data^{8,97,98}. BEESTS is based on the independent horse race model⁹⁹, which assumes that whether a response is successfully inhibited depends on the relative finishing times of a go and a stop runner. The runners are triggered by the go and stop stimuli, respectively. If, on a given stop-trial, the stop runner finishes first, response inhibition is successful. Conversely, if the go runner wins, a response is executed despite the stop-signal, resulting in a signal-response RT. BEESTS allows estimating the SSRT distribution (i.e., the finishing time distribution of the stop runner) which should be considered in its entirety (as opposed to means only). For example, distribution shapes may differ between experimental conditions even if mean SSRTs are the same. Disregarding the shape may lead to erroneous conclusions¹⁰⁰. Moreover, BEESTS can estimate the probability of go and stop trigger failures, the inability to start the go and stop runners, respectively, which may bias results^{8,101}. For example, if ignored, stop trigger failures may lead to overestimation of SSRTs¹⁰².

In the BEESTS approach, the finishing times of the go and stop runners are modeled as ex-Gaussian distributions with parameters μ , σ , and τ ⁹⁷. The first two parameters reflect the mean and standard deviation of the Gaussian component and the latter the exponential component, accounting for the long slow tail that is characteristic of RT distributions. The mean of the finishing time distributions (i.e., mean Go-RT and mean SSRT) is the sum of the μ and τ parameters (i.e., $\mu_{go} + \tau_{go}$ and $\mu_{stop} + \tau_{stop}$). To account for go and stop runner start deficiencies, we used an augmented version of the standard BEESTS that also estimates the parameters $P(\text{TF})$ and $P(\text{GF})$, the probability of triggering the stop and go runners, respectively^{8,101}.

After removing all choice errors on go-trials, the model was estimated separately for each experimental condition. To account for the nested data structure, we used hierarchical modeling¹⁰³. For signal response trials (i.e. stop-signal trials), the accuracy of responses with respect to the go stimulus was not recorded, so it was not possible to distinguish between correct and incorrect choices. It is therefore possible that stop-signal trials with incorrect choice data were included in the analysis. However, given the overall low error rate on go-trials, we did not expect the model parameters to be considerably biased by incorrect signal-response trials. Appendix 1 shows the model parametrization and the weakly informative hyperpriors that restricted the parameters to a plausible range. We used the Dynamic Models of Choice software¹⁰⁰ in the programming environment R (R Core Team, 2019) to fit the models. We assessed model convergence by visually inspecting the Markov chain Monte Carlo (MCMC) chains and by using univariate and multivariate proportional scale-reduction factors ($\hat{R} < 1.1$)^{104,105}. The model fits were evaluated using posterior predictive checks. Overall, they provided a good account of the data (see Appendix 1 for more details regarding the fitting procedure and model assessment).

Ethics statement. The study was approved by the local ethics committee of the Medical Faculty at Leipzig University (# 440/20-ck). All methods were performed in accordance with the relevant guidelines and regulations. All participants provided written informed consent.

Data availability

The data is freely available on OSF <https://osf.io/w5sry>.

Received: 23 March 2023; Accepted: 16 July 2023

Published online: 18 July 2023

References

1. Tiego, J., Testa, R., Bellgrove, M. A., Pantelis, C. & Whittle, S. A hierarchical model of inhibitory control. *Front. Psychol.* **9**, 1339 (2018).
2. Floden, D. & Stuss, D. T. Inhibitory control is slowed in patients with right superior medial frontal damage. *J. Cogn. Neurosci.* **18**, 1843–1849 (2006).
3. Obeso, I. et al. Deficits in inhibitory control and conflict resolution on cognitive and motor tasks in Parkinson's disease. *Exp. Brain Res.* **212**, 371–384 (2011).
4. Voon, V. & Dalley, J. W. Impulsive choice—Parkinson disease and dopaminergic therapy. *Nat. Rev. Neurol.* **7**, 541–542 (2011).
5. de Wit, F. R. C., Greer, L. L. & Jehn, K. A. The paradox of intragroup conflict: A meta-analysis. *J. Appl. Psychol.* **97**, 360–390 (2012).

6. Lipszyc, J. & Schachar, R. Inhibitory control and psychopathology: A meta-analysis of studies using the stop signal task. *J. Int. Neuropsychol. Soc.* **16**, 1064–1076 (2010).
7. Schachar, R. & Logan, G. D. Impulsivity and inhibitory control in normal development and childhood psychopathology. *Dev. Psychol.* **26**, 710–720 (1990).
8. Matzke, D., Hughes, M., Badcock, J. C., Michie, P. & Heathcote, A. Failures of cognitive control or attention? The case of stop-signal deficits in schizophrenia. *Atten. Percept. Psychophys.* **79**, 1078–1086 (2017).
9. Weigard, A., Heathcote, A., Matzke, D. & Huang-Pollock, C. Cognitive modeling suggests that attentional failures drive longer stop-signal reaction time estimates in attention deficit/hyperactivity disorder. *Clin. Psychol. Sci.* **7**, 856–872 (2019).
10. Verbruggen, F. *et al.* A consensus guide to capturing the ability to inhibit actions and impulsive behaviors in the stop-signal task. *Elife* <https://doi.org/10.7554/elife.46323> (2019).
11. Logan, G. D. The point of no return: A fundamental limit on the ability to control thought and action. *Q. J. Exp. Psychol.* **68**, 833–857 (2015).
12. Verbruggen, F. & Logan, G. D. Evidence for capacity sharing when stopping. *Cognition* **142**, 81–95 (2015).
13. Verbruggen, F. & Logan, G. D. Models of response inhibition in the stop-signal and stop-change paradigms. *Neurosci. Biobehav. Rev.* <https://doi.org/10.1016/j.neubiorev.2008.08.014> (2009).
14. Friehs, M. A. M. A. *et al.* Effective gamification of the stop-signal task: Two controlled laboratory experiments. *JMIR Serious Games* <https://doi.org/10.2196/17810> (2020).
15. Schroeder, P. A., Lohmann, J. & Ninaus, M. Preserved inhibitory control deficits of overweight participants in a gamified stop-signal task: Experimental study of validity. *JMIR Serious Games* <https://doi.org/10.2196/25063> (2021).
16. Gallagher, R., Kessler, K., Bramham, J., Dechant, M. & Friehs, M. A. A proof-of-concept study exploring the effects of impulsivity on a gamified version of the stop-signal task in children. *Front. Psychol.* **14**, 1068229 (2023).
17. Klock, A. C. T., Gasparini, I., Pimenta, M. S. & Hamari, J. Tailored gamification: A review of literature. *Int. J. Hum.-Comput. Stud.* **144**, 102495 (2020).
18. Wiley, K., Vedress, S. & Mandryk, L., Regan. How points and theme affect performance and experience in a gamified cognitive task. *Proc. Conf. Hum. Factors Comput. Syst. CHI 2020* (2020).
19. Wiley, K., Robinson, R. & Mandryk, R. L. The making and evaluation of digital games used for the assessment of attention: Systematic review. *JMIR Serious Games* **9**, e26449 (2021).
20. Luria, A. R. *Higher Cortical Functions in Man* (Springer Science & Business Media, 2012).
21. Aron, A. R., Robbins, T. W. & Poldrack, R. A. Inhibition and the right inferior frontal cortex: One decade on. *Trends Cogn. Sci.* <https://doi.org/10.1016/j.tics.2013.12.003> (2014).
22. Dambacher, F. *et al.* The role of right prefrontal and medial cortex in response inhibition: Interfering with action restraint and action cancellation using transcranial magnetic brain stimulation. *J. Cogn. Neurosci.* https://doi.org/10.1162/jocn_a_00595 (2014).
23. Depue, B. E., Orr, J. M., Smolker, H. R., Naaz, F. & Banich, M. T. The organization of right prefrontal networks reveals common mechanisms of inhibitory regulation across cognitive, emotional, and motor processes. *Cereb. Cortex* <https://doi.org/10.1093/cercor/bhu324> (2016).
24. Miller, E. K. & Cohen, J. D. An integrative theory of prefrontal cortex function. *Annu. Rev. Neurosci.* **24**, 167–202 (2001).
25. Callejas, A., Lupiáñez, J. & Tudela, P. The three attentional networks: On their independence and interactions. *Brain Cogn.* **54**, 225–227 (2004).
26. Curtis, C. E. & D'Esposito, M. Persistent activity in the prefrontal cortex during working memory. *Trends Cogn. Sci.* **7**, 415–423 (2003).
27. Silvers, J. A., Wager, T. D., Weber, J. & Ochsner, K. N. The neural bases of uninstructed negative emotion modulation. *Soc. Cogn. Affect. Neurosci.* **10**, 10–18 (2015).
28. Staudinger, M. R., Erk, S. & Walter, H. Dorsolateral prefrontal cortex modulates striatal reward encoding during reappraisal of reward anticipation. *Cereb. Cortex* **21**, 2578–2588 (2011).
29. Ochsner, K. N., Silvers, J. A. & Buhle, J. T. Functional imaging studies of emotion regulation: A synthetic review and evolving model of the cognitive control of emotion: Functional imaging studies of emotion regulation. *Ann. N. Y. Acad. Sci.* **1251**, E1–E24 (2012).
30. Krawczyk, D. C. Contributions of the prefrontal cortex to the neural basis of human decision making. *Neurosci. Biobehav. Rev.* **26**, 631–664 (2002).
31. Hornberger, M. & Bertoux, M. Right lateral prefrontal cortex—Specificity for inhibition or strategy use? (2015) <https://doi.org/10.1093/brain/awv027>.
32. Fregni, F. *et al.* Cortical stimulation of the prefrontal cortex with transcranial direct current stimulation reduces cue-provoked smoking craving: A randomized, sham-controlled study. *J. Clin. Psychiatry* **69**, 32–40 (2008).
33. Goldman, R. L. *et al.* Prefrontal cortex transcranial direct current stimulation (tDCS) temporarily reduces food cravings and increases the self-reported ability to resist food in adults with frequent food craving. *Appetite* **56**, 741–746 (2011).
34. Aron, A. R., Robbins, T. W. & Poldrack, R. A. Inhibition and the right inferior frontal cortex. *Trends Cogn. Sci.* <https://doi.org/10.1016/j.tics.2004.02.010> (2004).
35. Hampshire, A., Chamberlain, S. R., Monti, M. M., Duncan, J. & Owen, A. M. The role of the right inferior frontal gyrus: Inhibition and attentional control. *Neuroimage* **50**, 1313–1319 (2010).
36. Aron, A. R., Fletcher, P. C., Bullmore, E. T., Sahakian, B. J. & Robbins, T. W. Stop-signal inhibition disrupted by damage to right inferior frontal gyrus in humans. *Nat. Neurosci.* **6**, 115–116 (2003).
37. Erika-Florence, M., Leech, R. & Hampshire, A. A functional network perspective on response inhibition and attentional control. *Nat. Commun.* **5**, 4073 (2014).
38. Choo, Y., Matzke, D., Bowren, M. D., Tranel, D. & Wessel, J. R. Right inferior frontal gyrus damage is associated with impaired initiation of inhibitory control, but not its implementation. *Elife* **11**, e79667 (2022).
39. Allen, C., Singh, K. D., Verbruggen, F. & Chambers, C. D. Evidence for parallel activation of the pre-supplementary motor area and inferior frontal cortex during response inhibition: A combined MEG and TMS study. *R. Soc. Open Sci.* **5**, 171369 (2018).
40. Jha, M. *et al.* Neuropsychological and imaging profile of patients with Parkinson's disease and freezing of gait. *Parkinsonism Relat. Disord.* **21**, 1184–1190 (2015).
41. Swann, N. C. *et al.* Roles for the pre-supplementary motor area and the right inferior frontal gyrus in stopping action: Electrophysiological responses and functional and structural connectivity. *Neuroimage* **59**, 2860–2870 (2012).
42. Verbruggen, F. & Logan, G. D. Response inhibition in the stop-signal paradigm Successful stopping: Inhibition and performance monitoring. *Trends Cogn. Sci.* <https://doi.org/10.1016/j.tics.2008.07.005> (2008).
43. Chambers, C. D. *et al.* Dissociable mechanisms of cognitive control in prefrontal and premotor cortex. *J. Neurophysiol.* <https://doi.org/10.1152/jn.00685.2007> (2007).
44. Chambers, C. D. *et al.* Executive 'brake failure' following deactivation of human frontal lobe. *J. Cogn. Neurosci.* <https://doi.org/10.1162/089892906775990606> (2006).
45. Obeso, I., Robles, N., Marrón, E. M. & Redolar-Ripoll, D. Dissociating the role of the pre-SMA in response inhibition and switching: A combined online and offline TMS approach. *Front. Hum. Neurosci.* <https://doi.org/10.3389/fnhum.2013.00150> (2013).

46. Lee, H. W. *et al.* Roles of the pre-SMA and rIFG in conditional stopping revealed by transcranial magnetic stimulation. *Behav. Brain Res.* <https://doi.org/10.1016/j.bbr.2015.08.024> (2016).
47. Upton, D. J., Cooper, N. R., Laycock, R., Croft, R. J. & Fitzgerald, P. B. A combined rTMS and ERP investigation of dorsolateral prefrontal cortex involvement in response inhibition. *Clin. EEG Neurosci.* <https://doi.org/10.1177/155005941004100304> (2010).
48. Friehs, M. A., Dechant, M., Vedress, S., Frings, C. & Mandryk, R. L. Shocking advantage! Improving digital game performance using non-invasive brain stimulation. *Int. J. Hum. Comput. Stud.* <https://doi.org/10.1016/j.ijhcs.2020.102582> (2020).
49. Kirsten, H., Dechant, M., Gibbons, H. & Friehs, M. A. Tasting inhibition: A proof-of-concept study of the food stop-signal game. In *Progress in Brain Research* (Elsevier, 2023). <https://doi.org/10.1016/bs.pbr.2022.12.002>.
50. Schroeder, P. A., Mayer, K., Wirth, R. & Svaldi, J. Playing with temptation: Stopping abilities to chocolate are superior, but also more extensive. *Appetite* **181**, 106383 (2023).
51. Rouder, J. N., Morey, R. D., Verhagen, J., Province, J. M. & Wagenmakers, E. J. Is there a free lunch in inference?. *Top. Cogn. Sci.* <https://doi.org/10.1111/tops.12214> (2016).
52. Numssen, O., Van Der Burght, C. L. & Hartwigsen, G. Revisiting the focality of non-invasive brain stimulation—Implications for studies of human cognition. *Neurosci. Biobehav. Rev.* **149**, 105154 (2023).
53. Krause, B. & Cohen Kadosh, R. Not all brains are created equal: the relevance of individual differences in responsiveness to transcranial electrical stimulation. *Front. Syst. Neurosci.* **8**, (2014).
54. Bergmann, T. O. & Hartwigsen, G. Inferring causality from noninvasive brain stimulation in cognitive neuroscience. *J. Cogn. Neurosci.* https://doi.org/10.1162/jocn_a_01591 (2020).
55. Silvanto, J., Bona, S., Marelli, M. & Cattaneo, Z. On the mechanisms of transcranial magnetic stimulation (TMS): How brain state and baseline performance level determine behavioral effects of TMS. *Front. Psychol.* **9**, 741 (2018).
56. Schwarzkopf, D. S., Silvanto, J. & Rees, G. Stochastic resonance effects reveal the neural mechanisms of transcranial magnetic stimulation. *J. Neurosci.* <https://doi.org/10.1523/JNEUROSCI.4863-10.2011> (2011).
57. Hartwigsen, G. Flexible redistribution in cognitive. *Networks* <https://doi.org/10.1016/j.tics.2018.05.008> (2018).
58. Friehs, M. A., Brauner, L. & Frings, C. Dual-tDCS over the right prefrontal cortex does not modulate stop-signal task performance. *Exp. Brain Res.* <https://doi.org/10.1007/s00221-020-05995-5> (2021).
59. Friehs, M. A., Frings, C. & Hartwigsen, G. Effects of single-session transcranial direct current stimulation on reactive response inhibition. *Neurosci. Biobehav. Rev.* <https://doi.org/10.1016/j.neubiorev.2021.07.013> (2021).
60. Friehs, M. A., Whelan, E., Gildenpenning, I., Krause, D. & Weigelt, M. Stimulating performance: A scoping review on transcranial electrical stimulation effects on olympic sports. *Psychol. Sport Exerc.* **59**, 102130 (2022).
61. Friehs, M. A., Klaus, J., Singh, T., Frings, C. & Hartwigsen, G. Perturbation of the right prefrontal cortex disrupts interference control. *Neuroimage* <https://doi.org/10.1016/j.neuroimage.2020.117279> (2020).
62. Brownsett, S. L. E. *et al.* Cognitive control and its impact on recovery from aphasic stroke. *Brain* <https://doi.org/10.1093/brain/awt289> (2014).
63. Geranmayeh, F., Chau, T. W., Wise, R. J. S., Leech, R. & Hampshire, A. Domain-general subregions of the medial prefrontal cortex contribute to recovery of language after stroke. *Brain* <https://doi.org/10.1093/brain/awx134> (2017).
64. Turner, G. R., McIntosh, A. R. & Levine, B. Prefrontal compensatory engagement in TBI is due to altered functional engagement of existing networks and not functional reorganization. *Front. Syst. Neurosci.* <https://doi.org/10.3389/fnsys.2011.00009> (2011).
65. Geranmayeh, F., Brownsett, S. L. E. & Wise, R. J. S. Task-induced brain activity in aphasic stroke patients: What is driving recovery?. *Brain* **137**, 2632–2648 (2014).
66. Murphy, T. H. & Corbett, D. Plasticity during stroke recovery: From synapse to behaviour. *Nat. Rev. Neurosci.* **10**, 861–872 (2009).
67. Nudo, R. Adaptive plasticity in motor cortex: Implications for rehabilitation after brain injury. *J. Rehabil. Med.* **35**, 7–10 (2003).
68. Hartwigsen, G. & Silvanto, J. Noninvasive brain stimulation: Multiple effects on cognition. *Neuroscientist* <https://doi.org/10.1177/10738584221113806> (2022).
69. Lee, M. D. & Wagenmakers, E.-J. *Bayesian Cognitive Modeling: A Practical Course* (Cambridge University Press, 2014).
70. Bergmann, T. O., Karabanov, A., Hartwigsen, G., Thielscher, A. & Siebner, H. R. Combining non-invasive transcranial brain stimulation with neuroimaging and electrophysiology: Current approaches and future perspectives. *Neuroimage* **140**, 4–19 (2016).
71. Bergmann, T. O. *et al.* Concurrent TMS-fMRI for causal network perturbation and proof of target engagement. *Neuroimage* **237**, 118093 (2021).
72. Duecker, F. & Sack, A. T. Rethinking the role of sham TMS. *Front. Psychol.* **6**, (2015).
73. Duecker, F., De Graaf, T. A., Jacobs, C. & Sack, A. T. Time- and task-dependent non-neural effects of real and sham TMS. *PLoS ONE* **8**, e73813 (2013).
74. Parkin, B. L., Ekhtiari, H. & Walsh, V. F. Non-invasive human brain stimulation in cognitive neuroscience: A primer. *Neuron* **87**, 932–945 (2015).
75. Faul, F., Erdfelder, E., Lang, A.-G. & Buchner, A. G*Power: A flexible statistical power analysis program for the social, behavioral, and biomedical sciences. *Behav. Res. Methods* **39**, 175–191 (2007).
76. Kimbrell, T. A. *et al.* Left prefrontal-repetitive transcranial magnetic stimulation (rTMS) and regional cerebral glucose metabolism in normal volunteers. *Psychiatry Res. Neuroimaging* **115**, 101–113 (2002).
77. Hartwigsen, G. *et al.* Left dorsal premotor cortex and supramarginal gyrus complement each other during rapid action reprogramming. *J. Neurosci.* **32**, 16162–16171 (2012).
78. Ward, N. S. *et al.* Low-frequency transcranial magnetic stimulation over left dorsal premotor cortex improves the dynamic control of visuospatially cued actions. *J. Neurosci.* **30**, 9216–9223 (2010).
79. Van Der Plas, M., Braun, V., Stauch, B. J. & Hanslmayr, S. Correction: Stimulation of the left dorsolateral prefrontal cortex with slow rTMS enhances verbal memory formation. *PLoS Biol.* **19**, e3001451 (2021).
80. Fitzgerald, P. Intensity-dependent effects of 1 Hz rTMS on human corticospinal excitability. *Clin. Neurophysiol.* **113**, 1136–1141 (2002).
81. Speer, A. M. *et al.* Intensity-dependent regional cerebral blood flow during 1-Hz repetitive transcranial magnetic stimulation (rTMS) in healthy volunteers studied with H215O positron emission tomography: i. Effects of primary motor cortex rTMS. *Biol. Psychiatry* **54**, 818–825 (2003).
82. Criaud, M. & Boulinguez, P. Have we been asking the right questions when assessing response inhibition in go/no-go tasks with fMRI? A meta-analysis and critical review. *Neurosci. Biobehav. Rev.* **37**, 11–23 (2013).
83. Hung, Y., Gaillard, S. L., Yarmak, P. & Arsalidou, M. Dissociations of cognitive inhibition, response inhibition, and emotional interference: Voxelwise ALE meta-analyses of fMRI studies. *Hum. Brain Mapp.* **39**, 4065–4082 (2018).
84. Rae, C. L., Hughes, L. E., Anderson, M. C. & Rowe, J. B. The prefrontal cortex achieves inhibitory control by facilitating subcortical motor pathway connectivity. *J. Neurosci.* <https://doi.org/10.1523/JNEUROSCI.3093-13.2015> (2015).
85. Swick, D., Ashley, V. & Turken, U. Are the neural correlates of stopping and not going identical? Quantitative meta-analysis of two response inhibition tasks. *Neuroimage* **56**, 1655–1665 (2011).
86. Zhang, R., Geng, X. & Lee, T. M. C. Large-scale functional neural network correlates of response inhibition: An fMRI meta-analysis. *Brain Struct. Funct.* **222**, 3973–3990 (2017).

87. Kuhnke, P., Meyer, L., Friederici, A. D. & Hartwigsen, G. Left posterior inferior frontal gyrus is causally involved in reordering during sentence processing. *Neuroimage* <https://doi.org/10.1016/j.neuroimage.2017.01.013> (2017).
88. Rossi, S. *et al.* Safety, ethical considerations, and application guidelines for the use of transcranial magnetic stimulation in clinical practice and research. *Clin. Neurophysiol.* <https://doi.org/10.1016/j.clinph.2009.08.016> (2009).
89. Rossini, P. M. *et al.* Non-invasive electrical and magnetic stimulation of the brain, spinal cord, roots and peripheral nerves: Basic principles and procedures for routine clinical and research application: An updated report from an I.F.C.N. Committee. (2015) <https://doi.org/10.1016/j.clinph.2015.02.001>.
90. Saturino, G. B., Siebner, H. R., Madsen, K. H. & Thielscher, A. Feasibility of focused multichannel transcranial current stimulation. In *10th Forum of Neuroscience (FENS)* (2016).
91. Thielscher, A., Antunes, A. & Saturnino, G. B. Field modeling for transcranial magnetic stimulation: A useful tool to understand the physiological effects of TMS? In *Proceedings of the Annual International Conference of the IEEE Engineering in Medicine and Biology Society, EMBS* (2015). <https://doi.org/10.1109/EMBC.2015.7318340>.
92. Dahnke, R., Yotter, R. A. & Gaser, C. Cortical thickness and central surface estimation. *Neuroimage* **65**, 336–348 (2013).
93. Numssen, O. *et al.* Efficient high-resolution TMS mapping of the human motor cortex by nonlinear regression. *Neuroimage* **245**, 118654 (2021).
94. Weise, K. *et al.* Precise motor mapping with transcranial magnetic stimulation. *Nat. Protoc.* <https://doi.org/10.1038/s41596-022-00776-6> (2022).
95. Bowey, J. T. & Mandryk, R. L. Those are not the stories you are looking for: Using text prototypes to evaluate game narratives early. In *CHI PLAY 2017—Proceedings of the Annual Symposium on Computer–Human Interaction in Play* (2017). <https://doi.org/10.1145/3116595.3116636>.
96. Bowey, J. T., Friehs, M. A. & Mandryk, R. L. Red or blue pill. In *Proceedings of the 14th International Conference on the Foundations of Digital Games—FDG '19* 1–11 (ACM Press, 2019). <https://doi.org/10.1145/3337722.3337734>.
97. Matzke, D. Release the BEESTS: Bayesian estimation of Ex-Gaussian STop-Signal reaction time distributions. *Front. Psychol.* **4**, (2013).
98. Matzke, D., Dolan, C. V., Logan, G. D., Brown, S. D. & Wagenmakers, E.-J. Bayesian parametric estimation of stop-signal reaction time distributions. *J. Exp. Psychol. Gen.* **142**, 1047–1073 (2013).
99. Matzke, D., Verbruggen, F. & Logan, G. D. The stop-signal paradigm. In *Stevens' Handbook of Experimental Psychology and Cognitive Neuroscience* (ed. Wixted, J. T.) 1–45 (Wiley, 2018). <https://doi.org/10.1002/9781119170174.epcn510>.
100. Heathcote, A. *et al.* Dynamic models of choice. *Behav. Res. Methods* **51**, 961–985 (2019).
101. Matzke, D., Curley, S., Gong, C. Q. & Heathcote, A. Inhibiting responses to difficult choices. *J. Exp. Psychol. Gen.* **148**, 124–142 (2019).
102. Band, G. P. H., van der Molen, M. W. & Logan, G. D. Horse-race model simulations of the stop-signal procedure. *Acta Psychol. (Amst.)* **112**, 105–142 (2003).
103. Efron, B. & Morris, C. Stein's paradox in statistics. *Sci. Am.* **236**, 119–127 (1977).
104. Brooks, S. P. & Gelman, A. General methods for monitoring convergence of iterative simulations. *J. Comput. Graph. Stat.* **7**, 434–455 (1998).
105. Gelman, A. & Rubin, D. B. Inference from iterative simulation using multiple sequences. *Stat. Sci.* **7**, (1992).

Author contributions

M.F., G.H. and C.F. were involved in conceptualization. M.F., D.M., M.C.D., and O.N. were involved in creating the methodology and formal analysis. M.F., M.C.D. and O.N. were responsible for the visualizations. M.F. and J.S. were involved in the investigation itself. All authors contributed to writing the original draft as well as review editing.

Funding

Open Access funding enabled and organized by Projekt DEAL. MF was supported by the German Research Foundation (FR4485/1-1). GH was also supported by the German Research Foundation (HA 6314/4-2 and HA 6314/9-1). GH and MF were supported by the Max Planck Society. DM and MCD are supported by a Vidi grant (VI.Vidi.191.091) from the Dutch Research Council (NWO).

Competing interests

The authors declare no competing interests.

Additional information

Supplementary Information The online version contains supplementary material available at <https://doi.org/10.1038/s41598-023-38841-z>.

Correspondence and requests for materials should be addressed to M.A.F.

Reprints and permissions information is available at www.nature.com/reprints.

Publisher's note Springer Nature remains neutral with regard to jurisdictional claims in published maps and institutional affiliations.



Open Access This article is licensed under a Creative Commons Attribution 4.0 International License, which permits use, sharing, adaptation, distribution and reproduction in any medium or format, as long as you give appropriate credit to the original author(s) and the source, provide a link to the Creative Commons licence, and indicate if changes were made. The images or other third party material in this article are included in the article's Creative Commons licence, unless indicated otherwise in a credit line to the material. If material is not included in the article's Creative Commons licence and your intended use is not permitted by statutory regulation or exceeds the permitted use, you will need to obtain permission directly from the copyright holder. To view a copy of this licence, visit <http://creativecommons.org/licenses/by/4.0/>.

© The Author(s) 2023